Fluorine redistribution and incorporation during solid phase epitaxy of preamorphized Si

M. Mastromatteo, D. De Salvador, E. Napolitani,* F. Panciera,† G. Bisognin, and A. Carnera
MATIS-IMM-CNR and Dipartimento di Fisica, Università di Padova, Via Marzolo 8, I-35131 Padova, Italy

G. Impellizzeri, S. Mirabella, and F. Priolo
MATIS-IMM-CNR and Dipartimento di Fisica e Astronomia, Università di Catania, Via S. Sofia, I-95123 Catania, Italy
(Received 31 March 2010; revised manuscript received 2 October 2010; published 26 October 2010)

The redistribution of fluorine during solid phase epitaxial regrowth (SPER) of preamorphized Si has been experimentally investigated, explained, and simulated, for different F concentrations and temperatures. We demonstrate, by a detailed analysis and modeling of F secondary ion mass spectrometry chemical-concentration profiles, that F segregates in amorphous Si during SPER by splitting in three possible states: (i) a diffusive one that migrates in amorphous Si; (ii) an interface segregated state evidenced by the presence of a F accumulation peak at the amorphous-crystal interface; (iii) a clustered F state. The interplay among these states and their roles in the F incorporation into crystalline Si are fully described. It is shown that diffusive F migrates by a trap limited diffusion mechanism and also interacts with the advancing interface by a sticking-release dynamics that regulates the amount of F segregated at the interface. We demonstrate that this last quantity determines the regrowth rate through an exponential law. On the other hand we show that neither the diffusive F nor the one segregated at the interface can directly incorporate into the crystal but F has to cluster in the amorphous phase before being incorporated in the crystal, in agreement with recent experimental observations. The trends of the model parameters as a function of the temperature are shown and discussed obtaining a clear energetic scheme of the F redistribution and incorporation in preamorphized Si. The above physical understanding and the model could have a strong impact on the use of F as a tool for optimizing the doping profiles in the fabrication of ultrashallow junctions.

DOI: 10.1103/PhysRevB.82.155323 PACS number(s): 81.15.Np, 61.72.uf, 64.75.Jk, 66.30.J−

I. INTRODUCTION

The redistribution of impurities during phase transitions is a widely studied phenomenon that has a great relevance in many fields and especially in microelectronics. The realization of ultrashallow junctions (USJs) with abrupt profiles and high electrical activation has become an important technological challenging task.[1] One of the most promising methods to create USJs consists in introducing dopants, for example, B in *p*-type junctions, by ion implantation in preamorphized Si substrates.[2,3] Subsequently, the substrate is recrystallized by solid phase epitaxial regrowth (SPER).[4] Such process allows very high concentration of electrically active dopants, far above equilibrium,[5] and leaves all the implantation-induced defects beyond the original amorphous-crystal (a-c) interface. However these defects, called end-of-range (EOR) defects,[6] release self-interstitials upon further thermal annealing that diffuse toward the surface[7] and interact with B, causing the well-known transient-enhanced diffusion (TED) and the formation of B-interstitials clusters. Both phenomena are detrimental, spreading the junction and deteriorating the electrical activity of the dopant.[8,9]

It is possible to reduce or even eliminate TED if C or F are introduced by ion implantation between the dopants and the EOR defects since these elements in Si act as traps for self-interstitials.[10–16] In particular, F segregation during the amorphous-crystalline transition became recently an interesting case of study as the chemical profile of F after SPER, as well as the phenomena occurring during SPER, have a strong impact on the efficiency of F in controlling the doping profiles. F incorporation during SPER of Si,[17] F diffusion in amorphous Si (a-Si) (Ref. 18) and F segregation occurring at the a-c interface[19] were recently studied but a full comprehension of the processes involved in the F redistribution during SPER is still lacking.

In fact, the solution of this technological issue passes through the understanding of a very intriguing and complex physical problem, as, in principle, many phenomena might interplay to determine the impurity redistribution of F, such as: (i) the impurity segregation, (ii) the effect of the impurity on phase transition velocity, (iii) the impurity diffusion in the amorphous phase, and (iv) the precipitation of impurities in the bulk phases or at the interface and its influence on the above phenomena.

(i) The segregation of impurities in Si has been usually described by a first-order kinetic model[20] yielding for the total interface transport flux $f=h(C_1\text{-}C_2\ m)$ with h the transport coefficient, C_1 and C_2 the impurity concentrations at the two sides of the interface that separates the two phases and $m=C_1^*/C_2^*$ the equilibrium segregation coefficient, i.e., the ratio of the equilibrium solid solubilities in the two phases (C^*). The F segregation at the a-c interface is different with respect to the above classic model for a solute redistribution during solidification[21] because the segregation coefficient is observed to change with depth, as previously shown in Ref. 19. Nevertheless no modeling attempt going beyond the first-order segregation theory was tried[22,23] and as a consequence the available models are not able to reproduce correctly the time evolution of F segregation nor the F redistribution during SPER, and they do not give any microscopic description of the involved phenomena.

(ii) The SPER of Si in presence of dopants or impurities such as H, O, C, and F[4,24,25] or under stress[26–28] was inves-

tigated in the last 30 years. The SPER rate in intrinsic Si is described by an Arrhenius dependence on temperature with an activation energy of about 2.7 eV.[24,29] The most accepted description of SPER kinetics asserts that the regrowth starts from crystalline islands nucleation[26] at the a-c interface and it proceeds by migration of kinklike growth sites along [110] ledges.[30] The effect of doping on SPER rate is well understood and is due to the charge state of defects involved in the regrowth. On the other hand little is known so far about the effect of inactive impurities, such as F, on the kinetics of the regrowth.[24] In particular, the activation energy of SPER in presence of F is observed to be slightly higher than in intrinsic Si (3.07 eV),[24] and Park[31] suggested that this is due to an immobilization of broken bonds by F, hindering the ledges motion and slowing down the SPER rate. However, Rudawski *et al.*[32] recently suggested that the nucleation kinetics are probably unaltered by electrically inactive species. They attributed the slowdown of SPER to the additional time needed to incorporate impurities that tend to cause local lattice distortions if not substitutionally incorporated but a relationship between the amount of impurities and the related distortions and slowdown of SPER has not been found yet. Recently, it was discovered that F dopes Si (Ref. 33) but not at levels high enough to influence the regrowth rate.[24]

(iii) F diffuses in a-Si with an activation energy of 2.2 eV (in a temperature range between 600 °C and 700 °C) (Ref. 18) but the microscopic mechanism driving F diffusion in a-Si is still unclear. Nash *et al.*[18] also observed immobile F in the vicinity of the F implant peak in a-Si and they suggested that some F is trapped at damage associated with ion implantation.

(iv) Recently, our group demonstrated by transmission electron microscopy (TEM) analyses that F clusters in a-Si into nanobubbles that are then incorporated in c-Si during SPER.[34] Moreover we demonstrated by means of x-ray absorption fine structure analysis that these bubbles are filled with SiF_4 molecules.[35] Therefore, F clustering in a-Si has to be considered and described in order to fully understand F diffusion in a-Si and F incorporation in c-Si during SPER.

In this paper we report a broad experimental investigation on the redistribution of the chemical profile of F in Si during SPER. We propose a model able to predict the evolution of F during SPER starting from the as-implanted profile, combining together all the phenomena [(i)–(iv)] described above. The model, together with its physical understanding, should improve the knowledge and the use of F as a tool for optimizing the doping profiles in the fabrication of USJs. This kind of experimental approach and modelization might also be transferred with success in similar systems, where redistribution of impurities occurs during phase transitions.

II. EXPERIMENTAL

Si samples were amorphized from the surface to a depth of ~550 nm or ~1 μm by implanting Si^- (3×10^{15} ions/cm^2 at 250 keV plus 2×10^{15} ions/cm^2 at 40 keV or 3×10^{15} ions/cm^2 at 500 keV plus 2×10^{15} ions/cm^2 at 40 keV, respectively) at the liquid-nitrogen temperature. Several amorphized samples were enriched in F at different concentrations by ion implantation as described in Table I: low-concentration samples (LC), medium-concentration samples (MC), and high-concentration samples (HCa and HCb) with a F peak in the as-implanted sample at 1×10^{19} F/cm^3 (for LC), at 5×10^{19} F/cm^3 (for MC), and at 2.2×10^{20} F/cm^3 (for both HCa and HCb). In most cases multiple implants have been done. All the implanted samples were annealed at 450 °C for 30 min to sharpen the a-c interface without inducing SPER. Then the samples were partially or completely regrown by annealing them in N_2 atmosphere to characterize the SPER kinetics at three different temperatures: 580, 650, and 700 °C. The annealings at the lowest temperature were made in a conventional horizontal furnace with an accuracy of ±3 °C while the ones at higher temperatures were done by rapid thermal annealing with a Jipelec JetFirst 150 using 25 °C/s ramps and an accuracy of ±3.5 °C. The concentration depth profiles of F were obtained by secondary ions mass spectrometry (SIMS) using a CAMECA IMS-4f instrument, by collecting F^+ secondary ions while sputtering with a 3 keV O_2^+ beam.

TABLE I. List of F implants.

Sample	F implants
LC	1.08×10^{14} F/cm^2 at 130 keV+
	1.08×10^{14} F/cm^2 at 180 keV+
	2.4×10^{14} F/cm^2 at 250 keV
MC	5.4×10^{14} F/cm^2 at 130 keV+
	5.4×10^{14} F/cm^2 at 180 keV+
	1.2×10^{15} F/cm^2 at 250 keV
HCa	2.0×10^{15} F/cm^2 at 100 keV
HCb	3.0×10^{15} F/cm^2 at 65 keV+
	9.0×10^{14} F/cm^2 at 30 keV

III. EXPERIMENTAL RESULTS

Figure 1 reports the F profiles relative to the MC sample series both before (dotted line) and after partial SPER (continuous lines) obtained with different annealing times at 580 °C. Furthermore the a-c interface positions, valued as the interface peak centroids, are reported as vertical dashed lines. The figure shows a clear overview of the main features of the F redistribution during SPER. As the a-c interface moves with the annealing time due to the regrowth, F segregates in a-Si splitting in two components: a sharp peak segregated at the a-c interface and a diffusing tail in the residual amorphous region. On the crystalline side F is incorporated at a concentration about two orders of magnitude lower than F peak and the F incorporation continues to increase while the F peak seems to saturate. The F profile in c-Si does not change during SPER, showing that F diffusion in c-Si is negligible while the F diffusion in a-Si appears to be significant. It is worth noting that the F diffusivity in a-Si seems to be significantly higher close to the a-c interface than far from it. This last aspect is remarkable and will be discussed deeply

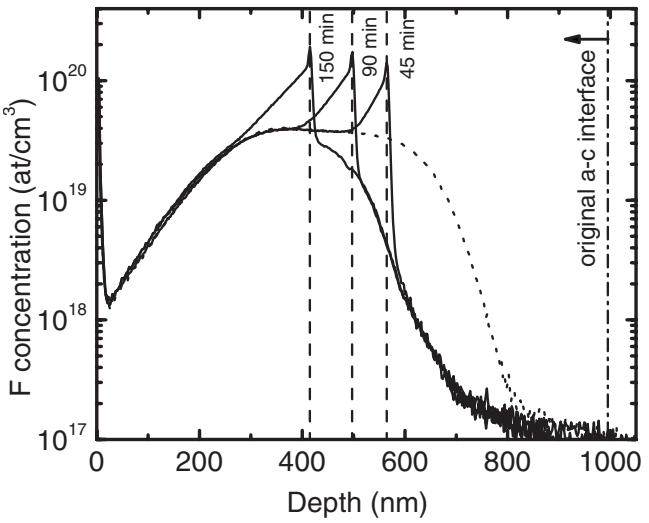

FIG. 1. F SIMS profiles of MC sample after implantation (dotted line) and after annealing at 580 °C (continuous lines) for different times (45, 90, and 150 min) performed in order to induce partial and complete regrowth. The a-c interface positions determined as the centroid of the segregated peak are also indicated by vertical dashed lines.

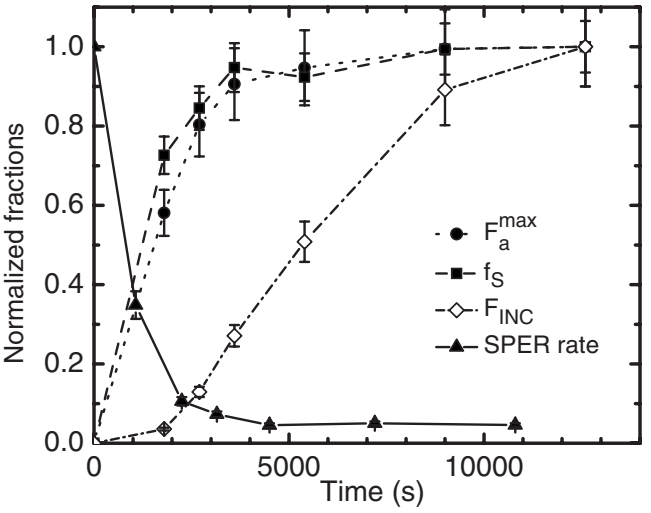

FIG. 3. The fraction of F_a^{max}, f_S, F_{INC}, and SPER rate with respect to their maximum value extracted from MC samples annealed at 580 °C are reported versus annealing time. Their maximum values are: 3.4×10^{19} at/cm^3 for F_a^{max} (closed circles), 9.3×10^{13} at/cm^2 for f_S (closed squares), 7.0×10^{19} at/cm^3 for F_{INC} (open diamonds), and 0.456 nm/s for SPER rate (closed triangles) (Ref. 27). The lines are only guides for eyes.

in Sec. IV B, together with the whole mechanism of F diffusion in a-Si during SPER.

In Fig. 2 a magnification of a segregation profile close to the a-c interface is shown. It is evident that three different zones should be considered corresponding to the regions of a three-phase system:[36,37] the amorphous phase, the crystalline phase and the region of the F peak segregated at the interface (i.e., the interface layer). We performed a first quantitative analysis by extracting some quantities directly from the profiles by simple extrapolation/integration operations. These quantities are: (i) the a-c interface depth, approximated as the peak centroid of the F concentration profile, (ii) the concentration of F in the amorphous phase at the a-c interface depth (F_a^{max}), assumed as the extrapolated F concentration, (iii) the incorporated F concentration in the crystalline phase at the a-c interface depth (F_{INC}), directly extracted from the completed regrown profile considering that F in c-Si has negligible diffusion, (iv) the F areal density of the a-c interface region (f_S), estimated by integrating the profile in the interface layer zone after subtraction of the F in amorphous and crystalline phase, and (v) the regrowth velocity estimated as the incremental ratio of the a-c interface positions and annealing times.

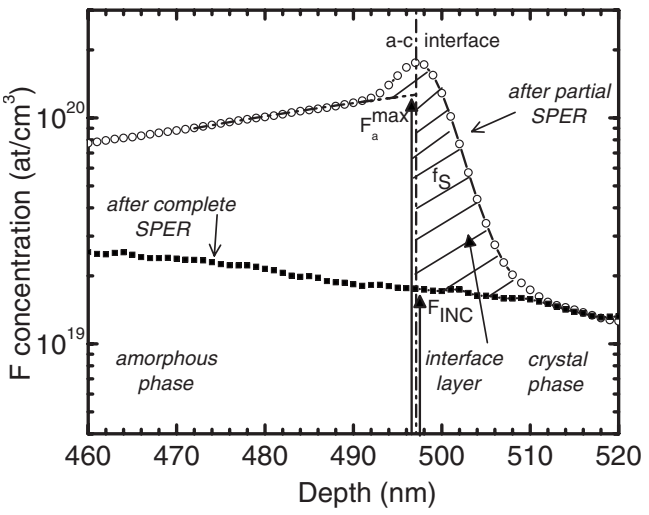

FIG. 2. Enlargement of the second F peak (open circles) of Fig. 1. The arrows indicate the F concentration in a-Si at the a-c interface (F_a^{max}), the F incorporated in c-Si concentration at the a-c interface (F_{INC}) while the F areal density of the a-c interface region (f_S), is represented by the cross-hatched area.

Figure 3 shows the last four quantities plotted versus time for the MC series at 580 °C. We normalized each quantity to its maximum value. As can be noted, F in amorphous (F_a^{max}) and F segregated in the peak (f_S) are very well correlated one another. We can also note that the SPER rate reaches a steady state with the same characteristic time of f_S and F_a^{max}, suggesting a strong correlation between these three quantities. Instead, F_{INC} is not correlated with any other one: when the other quantities have reached the saturation value, the F incorporated in the crystal still continues growing, nearly doubling its value before reaching the maximum. We observed similar trends in all other series of data. This confirms what can be argued by our recent observations,[34,35] i.e., that the incorporation mechanism is not governed solely by phenomena occurring at the a-c interface but a role is played by something else. According to Refs. 34 and 35, the additional phenomenon most probably is the clustering of F in bulk a-Si in nanobubbles filled with SiF_4, that are subsequently incorporated in c-Si. Figure 3 suggests that the clustering process of F continues to evolve with time in a-Si also after that diffusion and interface segregation have reached a steady state, and confirms that clustering has a dominant role in governing the incorporation process of F in c-Si. Conse-

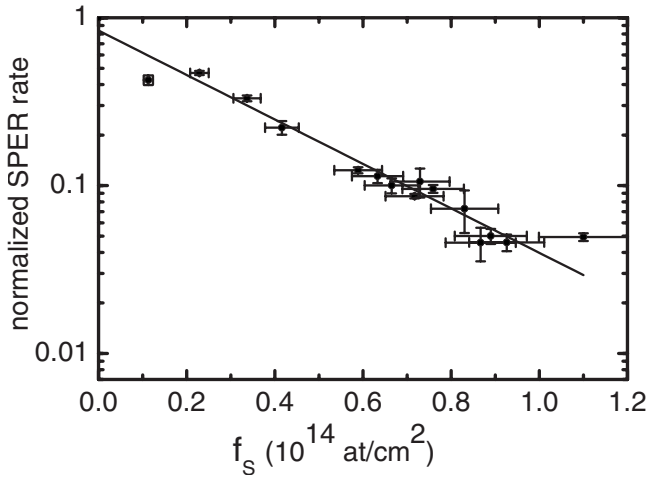

FIG. 4. Normalized SPER rate versus F areal density at the a-c interface. The continuous exponential line is described by Eq. (1).

quently, in order to satisfactorily describe the F incorporation in c-Si, we will assume that F in the amorphous phase can be distinguished in two different states, i.e., the F free to diffuse, hereafter called F_D, and the precipitated F, F_C, and we will consider the dynamics interplays between them.

In order to investigate the correlation between f_S and the SPER rate, we plotted in Fig. 4 the SPER rate normalized to the Si intrinsic SPER rate[24] versus the F areal density at the a-c interface for all the data available at 580 °C. Similar plots (not reported here) were achieved for the other temperatures. The f_S data reported in the plot are the mean values between two areal densities of peaks consecutive in time. It is possible to interpolate each set of data obtained at a fixed temperature with an exponential law

$$v = v_0 e^{-f_S/f_S^0}, \tag{1}$$

where v_0 is the SPER rate of intrinsic Si (see Ref. 24) and f_S^0 is a temperature dependent reduction coefficient of SPER rate due to f_S. The above phenomenological equation will be assumed for the modeling in the following section.

IV. RATE EQUATIONS MODEL

A quantitative description of all the phenomena evidenced above is fundamental to model the F redistribution during SPER, as they happen simultaneously and strongly influence one another. We have formulated physical models for each process and we coupled the rate equations of all the processes in an overall model. Then, for each annealing temperature, we fitted all the data simultaneously with a single set of physical parameters. In the following description each physical phenomenon involving F will be treated separately assuming that the others were already satisfactorily modeled. In this way, we will be able to discuss separately the physical origin of each phenomenon and the tests made in order to validate or discard the assumptions made. The model presented here is the most successful in term of chi-square minimization while keeping the number of free parameters as low as possible.

A. F clustering in a-Si

In Fig. 5 we show an attempt to simulate our profiles (LC and MC samples annealed at 580 °C) by assuming that clustering does not occur and that the diffusing F in a-Si incorporates into c-Si by a first-order kinetic model with a finite probability (1% at this temperature) of F incorporation in c-Si as suggested in Ref. 23. This simulation is compared to our best model obtained by including F clustering. It is evident that it is impossible to fit simultaneously and correctly the highest levels of F incorporated in LC [Fig. 5(a)] and MC [Fig. 5(b)] samples simply by assuming a classic first-order segregation whereas by including clustering it is possible to simulate satisfactorily the data. This fact should definitely convince that clustering has to be taken into account for an appropriate modeling. In the following, we will assume a perfect incorporation of the F clusters during the a-c interface motion and we will consider also that the clusters might dissolve before the arrival of the incoming a-c interface. Moreover, we assumed that the F diffusion in c-Si is negligible, as suggested by the experimental data (see Fig. 1). We modeled the clustering and incorporation through the following equations:

$$\frac{\partial[F_C]}{\partial t} = 4\pi\delta[N_0]D_{FD}[F_D] - \eta[F_C] \quad \text{for } x \le R \quad \text{and}$$

$$\frac{\partial[F_C]}{\partial t} = 0 \quad \text{for } x > R, \tag{2}$$

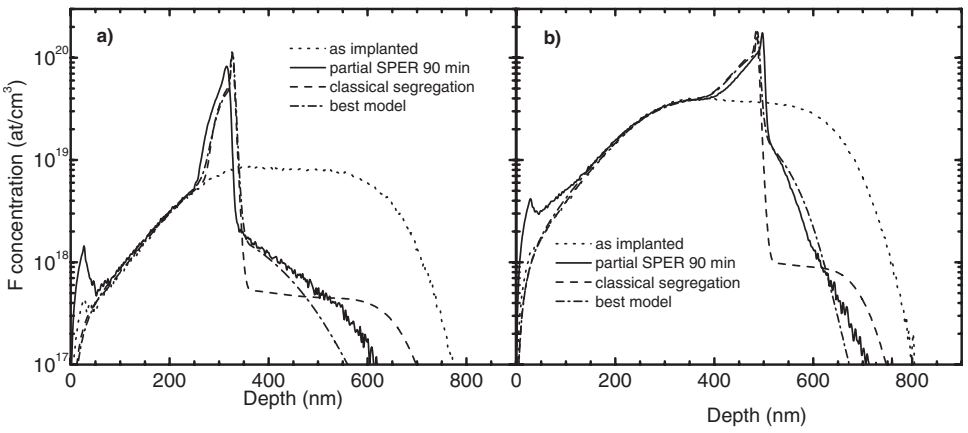

FIG. 5. F SIMS profiles for LC (a) and MC samples (b) just after implantation (dotted lines), and after SPER at 580 °C for 90 min (continuous line). Simulations using a classic segregation (dashed line) or our model based on the incorporation of clustered F (dashed-dotted line) are reported for comparison.

$$[F_{INC}] = [F_C] \quad \text{for } x \geq R. \tag{3}$$

In the above equations, as well as hereafter in the paper, square brackets represent concentrations, that are also a function of the depth x. The a-c interface moves with time and it is assumed at the depth $x=R$. The quantities $[F_C]$, $[F_D]$, and $[F_{INC}]$ have the same meaning as the analogous quantities in Sec. III, i.e., the concentrations of the F in clusters, the diffusive F and the F incorporated in c-Si respectively. We consider in Eq. (2) the clustering rate proportional to a capture radius δ, to the clusters concentration ($[N_0]$), to the F diffusivity (D_{FD}) in a-Si and to $[F_D]$. Moreover, $[F_C]$ can decrease with time due to the dissolution term that is the product of $[F_C]$ and the dissolution rate η. Equation (3) describes our assumption that all the clustered F is incorporated in c-Si during SPER. Before further discussing Eqs. (2) and (3), we report that by relaxing the hypothesis of full incorporation of clustered F [Eq. (3)] we had not obtained any improvement of the fit quality. Indeed, by making the fits while considering a partial incorporation allows to assert with a confidence level of 95%, according to the F-test,[38] that more than 93% of clustered F is incorporated into the crystal.

Besides all the above assumptions, we also considered that the capture radius δ may grow with the clustered F concentration due to the growth of the cluster size. We assumed that all F clusters have the shape of spherical nanobubbles (assumption supported by TEM measurements)[34] that are filled with a certain volume density of F, ρ. Assuming the average volume of the cluster, V_{cl}, equal to

$$V_{cl} = \frac{1}{\rho}\frac{[F_C]}{[N_0]} \tag{4}$$

we can define the capture radius δ by

$$\delta = a_0 + \left(\frac{3}{4\pi\rho}\frac{[F_C]}{[N_0]}\right)^{1/3}, \tag{5}$$

where a_0 is the initial capture radius (we fixed it to the first nearest-neighbor distance, 0.235 nm in Si).

In the present form the model has three physical parameters to describe the clustering phenomenon: the clustering nucleation density $[N_0]$, the volume density of F in the nanobubbles (ρ) and a dissolution rate η. These can be considered as a minimal set of parameters to describe the clustering probability, the growth of F capturing probability with cluster size and the possible re-emission of F from the clusters. Of course, the model is simplified since we assume a constant amount of nucleation sites, a single possible density of F in the nanobubbles during growth and a single release rate. Fitting attempts of the experimental data with the above model have demonstrated that these parameters are sufficient to describe the main features of the phenomenon producing satisfactory simulation results of the F incorporation in c-Si, as shown in Fig. 5 (dashed-dotted lines) and as will be shown also later.

Indeed, the fitting of the whole set of data shows a strong correlation between ρ and η parameters, hampering the convergence of both of them. We can fix physically reasonable values for the ρ parameter by estimating the maximum packing that the SiF_4 molecules can have in a spherical void: considering the reasonable molecule radius given the Si-F distance and the F covalent radius of 0.3 nm, a close packing with a density of 26.2 at/nm^3 can be estimated. Considering that statistically equivalent fits are obtained by fitting the data with ρ equal to 26.2 at/nm^3 or half of this value (the fit worsens with a significance level of only 62% according to F-test),[38] we decided to assume in the model the maximum packing condition, i.e., $\rho=26.2$ at/nm^3. On the other hand any other attempt to reduce the number of the parameters, such as, for example, by considering a constant capture radius, produced a significant worsening of the fitting (the fit with a constant capture radius decreases the fit quality with a significance level of about 100%).[38]

In order to have a deeper test on the proposed incorporation mechanism we tried to add other incorporation mechanisms of F in the crystal phase. First of all we considered the possibility that also diffusing F could be incorporated in c-Si, obtaining no improvement of the fits. More precisely, we can assert with a significance level of 95% (Ref. 38) that less than 0.25% of mobile F can directly incorporate in c-Si. A second possibility is that F segregated at the interface may incorporate directly into the crystal. We found that by adding this incorporation channel into the simulation the fit is unchanged at high concentrations and slightly improves for few spectra at low concentrations. According to the F-test[38] the improvement has a significance level of about 80% and we retain this not enough to justify the introduction of an additional parameter that instead should be further investigated with more data at low concentrations.

B. F diffusion in a-Si

As can be noted in Figs. 1 and 5, the F diffusivity in a-Si is not constant and it is much more pronounced close to the a-c interface than far from it. A clear evidence of this comes from the fact that the profiles far from the interface do not change with time before the arrival of the a-c interface, whereas close to the a-c interface there is a pronounced diffusing tail. This is quantitatively demonstrated in Fig. 6 where the dashed line, obtained with a best fit assuming a constant diffusion coefficient, fails in reproducing the experimental data (open circles). These considerations suggest that diffusion may be concentration dependent (i.e., it increases by increasing the concentration) or position dependent (i.e., it increases closer to the a-c interface). Indeed, from Fig. 5 it can be deduced that a pure concentration-dependent diffusion may be ruled out. In fact, considering the two chemical profiles at the same concentration level of 2×10^{19} at/cm^3, diffusion can be observed in one sample [Fig. 5(a)] but not in the other one [Fig. 5(b)] that was treated at the same temperature but implanted with a higher dose. We confirmed this qualitative idea by performing several simulations (not shown) with different functional dependences of F diffusivity against F concentration and no satisfactory agreement was reached simultaneously for all the samples. For example we attempted to fit the data by assuming a constant diffusivity (or a linear dependence of the diffusivity with $[F_D]$) obtaining a worsening of the fit with a significance level of 96% and about 100%, respectively, according to the F-test.[38]

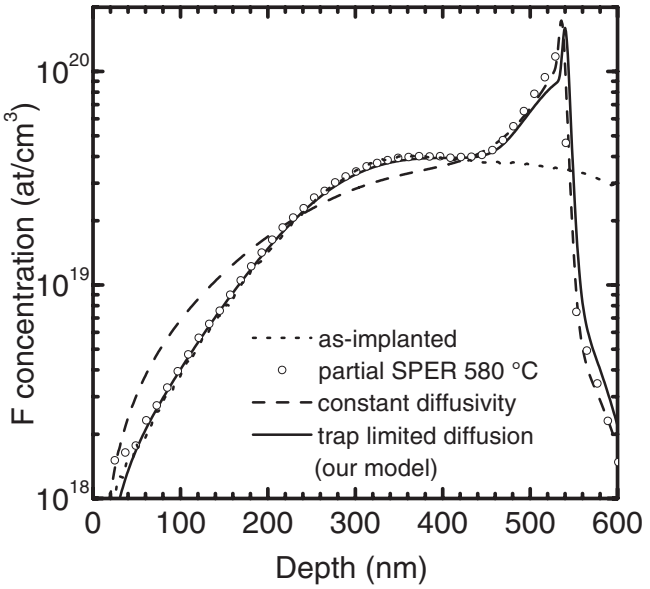

FIG. 6. F SIMS profiles of MC sample just after implantation (dotted line) and after annealing at 580 °C for 60 min (open circles). Simulations using constant diffusivity (dashed line) or our model based on a trap limited diffusion (continuous line) are reported for comparison.

A better description of the experimental data was reached after reasonably considering that there are a lot of defects in amorphous Si (Refs. 39–43) that can interact with the mobile F (i.e., trap-limited diffusion). F migrates and interacts with bulk defects, for example, dangling bonds that act as traps for F mobile atoms creating complexes and reducing the concentration of F able to migrate. The trapping reaction is described by

$$[\mathrm{F_I}] + [T] \leftrightarrow [FT], \tag{6}$$

where $\mathrm{F_I}$ represents the mobile F atoms in a-Si, T the traps, and FT the nondiffusive complex. We also introduce the parameter k regulating the equilibrium reaction according to the mass action law

$$\frac{[\mathrm{F_I}][T]}{[FT]} = k. \tag{7}$$

Therefore, the F diffusing state in a-Si ($\mathrm{F_D}$) is split in two parts: the mobile F ($\mathrm{F_I}$) and the F temporarily bonded to a trap (FT). The conservation of the total number of traps and diffusive fluorine gives the relations

$$[\mathrm{F_D}] = [\mathrm{F_I}] + [FT], \tag{8}$$

$$[T]_0 = [T] + [FT], \tag{9}$$

where $[T]_0$ is the total amount of traps before the interaction with F. Thus the diffusivity can be written as

$$D_{\mathrm{FD}} = D_{\mathrm{FI}} \frac{[\mathrm{F_I}]}{[\mathrm{F_D}]}, \tag{10}$$

where the $\mathrm{F_D}$ diffusivity (D_{FD}) is proportional to the $\mathrm{F_I}$ diffusivity (D_{FI}) multiplied by the fraction of moving F, i.e., $[\mathrm{F_I}]/[\mathrm{F_D}]$. This last ratio can be also expressed as a function of $[\mathrm{F_D}]$, $[T]_0$, and k by solving the system given by Eqs. (7)–(9) (not shown). As a consequence the diffusivity reaches a maximum value D_{FI} when the amount of F is much higher than the traps. On the contrary at low F concentrations the diffusivity is regulated by the equilibrium of reaction described by Eq. (6) that determines how much F is free to migrate at equilibrium.

In addition, we assumed that the advancing a-c interface is a perfect sink for the traps (i.e., traps capture length equal to zero) and consequently modifies the concentration of traps in such a way that $[T]_0$ is constant (equal to $[T]_{\mathrm{bulk}}$) except in the vicinity of the a-c interface, where traps concentration decays exponentially through the following equation:

$$[T]_0(x) = [T]_{\mathrm{bulk}}(1 - e^{(x-R)/\mu}), \tag{11}$$

where μ is the traps decay length at the a-c interface and R represents the a-c interface position. μ is an effective parameter taking into account the average diffusion length of traps that are supposed to be captured at the a-c interface. The above model for diffusion has four parameters (D_{FI}, k, $[T]_{\mathrm{bulk}}$, and μ) and is implemented with the boundary conditions that the sample surface is a perfect sink for mobile F while the advancing interface perfectly rejects the diffusive F.

In Fig. 6 we showed the F diffusion in a-Si obtained by the present model (continuous line). As can be noted, all the features of the diffusion are well reproduced and can be easily understood: the absence of the diffusion far from the interface is due to the fact that the F concentration is well below the trap concentration while close to the interface diffusion occurs thanks to the trap depletion. When the F concentration is higher than the trap concentration, all the traps are saturated so the F diffusion can occur also far from the a-c interface.

C. F segregation at the a-c interface and modeling of interface velocity

In this subsection we present the mathematical implementation of the model needed to simulate the areal density of F segregated at the a-c interface, f_{S}. Due to the phenomenological relation of this quantity with the regrowth velocity [see Eq. (1)], a good prediction of the evolution of f_{S} with time is crucial.

In our model the F segregation at the a-c interface is well reproduced by assuming a flux of F ($f_{\mathrm{S\_in}}$) coming from the amorphous phase during SPER

$$f_{\mathrm{S\_in}} = \alpha v[\mathrm{F_D}(R)]. \tag{12}$$

This flux is equal to the areal density of diffusing F that is interested by the regrowth per unit time $v[\mathrm{F_D}(R)]$, multiplied by a proportionality factor α that represents the fraction of such areal density that is trapped into the interface region (α can be thought as a segregation factor at the a-c interface).

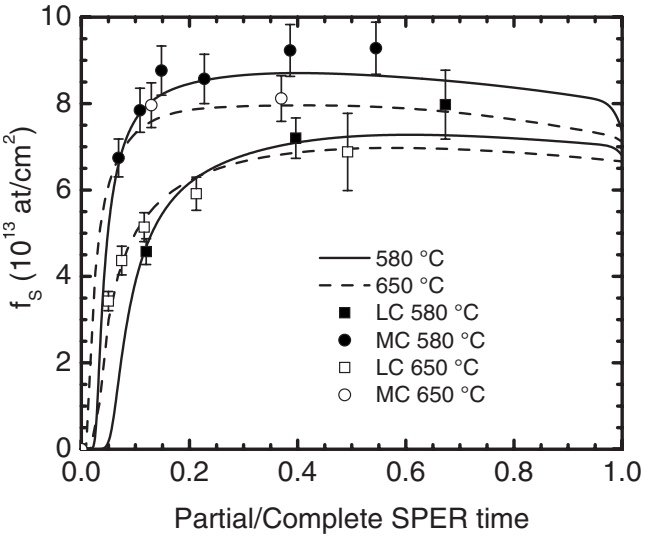

FIG. 7. F areal density at the a-c interface, f_S, of LC (squares) and MC (circles) for the temperatures of 580 °C (closed symbols) and 650 °C (open symbols) versus the normalized SPER time. Simulations are reported for comparison (dashed and continuous lines).

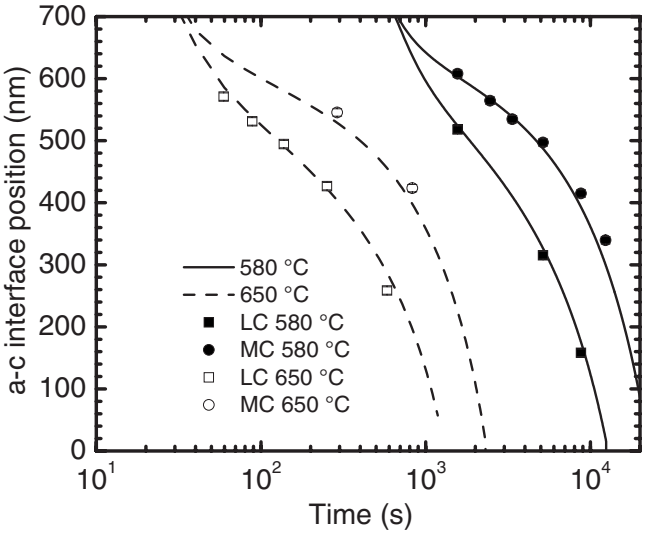

FIG. 8. The position of the a-c interface of LC (squares) and MC (circles) for the temperatures of 580 °C (closed symbols) and 650 °C (open symbols) versus time. Continuous and dotted lines are described by Eq. (1). The errors are less than the width of the dots.

It is also necessary to consider a second term that describes the releasing flux of F from the interface region to the amorphous bulk, f_{S_out}:

$$f_{S\_out} = \beta f_S \tag{13}$$

that is assumed to be simply proportional to the F amount into the interface region, f_S, being β a proportionality constant representing the dissolution rate of f_S.

Other terms were considered without success such as the possible release of F toward the crystalline phase and the possible reduction in F trapping at the interface region by approaching a saturation dose. The first one might be a possible channel of incorporation and the second one might be reasonably due to the finite availability of sites for the phase in a two-dimensional (2D) system. The first term was already statistically excluded in Sec. IV A. Considering the second term, we found that the $\chi 2$ of the fit increases for any finite 2D sites density demonstrating that also this additional parameter is useless. Thus, F segregation is described simply by a creation and a dissolution term through the following equation:

$$\frac{\partial f_S}{\partial t} = \alpha v[F_D(R)] - \beta f_S. \tag{14}$$

The good quality of the prediction of the evolution of f_S during SPER is shown in Fig. 7, where the F areal density f_S, is plotted versus the time fraction of the time for complete regrowth to allow a comparison between data sets at different temperatures. Continuous lines (simulation) and closed symbols (experimental) are used for series at 580 °C, and dashed lines (simulation) and open symbols (experimental) are used for series at 650 °C. We remind that a factor of ~16 exists between v_0 at the two considered temperatures. It is clear from the figure that the simulation data allow to perfectly account for the variation of f_S with time.

In Fig. 8 we show how the above model, through Eq. (1), allows also a fine prediction of the a-c interface positions. They are represented as continuous lines (simulation) and closed symbols (experimental) for series at 580 °C, and dashed lines (simulation) and open symbols (experimental) for series at 650 °C. A single value of f_S^0 coefficient for each temperature is able to reproduce well the interface positions within an average error of ~15 nm. It is worth noting that we also tried to add some other retardation effects such as exponential factors depending on the clustered and/or diffusive F at the a-c interface without any significant improvement of the fits. Such effects were therefore neglected.

D. Complete model

As previously discussed, the F retardation effect on the SPER rate, F clustering and diffusion in a-Si occur simultaneously and influence one another. All the equations introduced previously (see Secs. III and IV A–IV C) are coupled in an overall rate equations model able to fit all data sets at each SPER temperature.

The model is described by Eqs. (15)–(23), where F_D, F_C, F_{INC}, f_S, FT, and F_I are the diffusing F in a-Si, the clustered F, the F incorporated in c-Si, the F areal density at the a-c interface, the trapped F in a-Si and the mobile F in a-Si, respectively. The first three equations describe what happens in a-Si and the related incorporation of F in c-Si while the fourth describes the F exchanges at the a-c interface. The last four equations describe the trap limited diffusion. The main free, temperature-dependent, parameters of the model are N_0, η, α, β, and f_S^0, together with the free parameters governing the F diffusion coefficient in a-Si that are D_{FI}, $[T]_{bulk}$, μ, and the equilibrium constant of F-T reaction, k (for parameters description see Secs. III and IV).

$$\frac{\partial[\mathrm{F_D}]}{\partial t} = \frac{\partial}{\partial x} D_{\mathrm{FD}} \frac{\partial[\mathrm{F_D}]}{\partial x} - 4\pi[N_0]\left[a_0 + \left(\frac{3}{4\pi\rho}\frac{[\mathrm{F_C}]}{[N_0]}\right)^{1/3}\right] D_{\mathrm{FD}}[\mathrm{F_D}] + \eta[\mathrm{F_C}] \quad \text{for} \quad x \le R, \tag{15}$$

$$\frac{\partial[\mathrm{F_C}]}{\partial t} = 4\pi[N_0]\left[a_0 + \left(\frac{3}{4\pi\rho}\frac{[\mathrm{F_C}]}{[N_0]}\right)^{1/3}\right] D_{\mathrm{FD}}[\mathrm{F_D}] - \eta[\mathrm{F_C}] \quad \text{for} \quad x \le R \quad \text{and} \quad \frac{\partial[\mathrm{F_C}]}{\partial t} = 0 \quad \text{for} \quad x > R, \tag{16}$$

$$[\mathrm{F_{INC}}] = [\mathrm{F_C}] \quad \text{for} \quad x \ge R, \tag{17}$$

$$\frac{\partial f_S}{\partial t} = \alpha v[\mathrm{F_D}(R)] - \beta f_S, \tag{18}$$

$$v = v_0 e^{-f_S/f_S^0}, \tag{19}$$

$$D_{\mathrm{FD}} = D_{\mathrm{FI}} \frac{[\mathrm{F_I}]}{[\mathrm{F_D}]}, \tag{20}$$

$$\frac{[\mathrm{F_I}][T]}{[FT]} = k, \tag{21}$$

$$[\mathrm{F_D}] = [\mathrm{F_I}] + [FT], \tag{22}$$

$$[T]_0(x) = [T]_{\mathrm{bulk}}(1 - e^{(x-R)/\mu}). \tag{23}$$

The above system of differential equations was solved with a partially implicit algorithm implemented in an ANSI-C code created *ad hoc*. The code also manages the parameters optimization by means of chi-square minimization algorithm. For a given temperature and a given set of parameters all the profiles obtained with different annealing times are simulated starting from the respective as-implanted profiles. A cumulative chi-square is evaluated and used to perform a global optimization of the parameters based on all the information available at a given temperature.

All the three temperatures (580, 650, and 700 °C) were considered for the simulations. For each temperature three different starting (as-implanted) profiles were available with different F concentrations and, for each of the above as-implanted samples, the profiles relative to different (from 3 to 6) annealing times were measured and simulated. Summarizing, from the fitting procedure it was possible to fix the nine free parameters of the model describing the four different physical phenomena involved in the process: four parameters for the diffusion (D_{FI}, k, $[T]_{\mathrm{bulk}}$, μ), two for the segregation (α, β), one for the F effect on the SPER rate (f_s^0), and two for the clustering (N_0, η). The other parameter for the SPER rate, v_0, was fixed using literature values.[24]

V. RESULTS AND DISCUSSIONS

Figure 9 shows the entire set of SIMS profiles obtained at 650 °C. The as-implanted profiles are represented by dashed lines and the profiles partially or completely regrown are represented by dots for LC [Fig. 9(a)], MC [Fig. 9(b)], and HCb samples [Fig. 9(c)]. The best-fit profiles are also reported as continuous lines. The simulated profiles agree very well with the data and the same degree of accuracy were obtained also at 580 and 700 °C (not shown). The sharp peak segregated at the a-c interface and the diffusing tail in the amorphous bulk as well as the concentration levels of the incorporated F in c-Si are correctly described. We remind that the interface positions are predicted with an accuracy of 15 nm (see Fig. 8), which appears to be remarkable after considering that this variability might be justified by assuming an error on the process temperatures of 3–4 °C, that is close to the temperature accuracy of the annealing processes. The parameters relative to the best fits are reported in Table II for each of the three annealing temperatures and are discussed in the following. Some of them are reported also in Fig. 10 as Arrhenius plots together with their thermal activation energies.

Concerning the diffusion mechanism of F, we obtained that the diffusivity of mobile F, D_{FI}, varies with temperature with a prefactor of 0.13 $\mathrm{cm^2/s}$ and an activation energy of (2.2 ± 0.1) eV [see Fig. 10(a)]. Both of them are very similar to the F diffusion coefficient reported by Nash *et al.*[18] The other diffusion-related parameters ($[T]_{\mathrm{bulk}}$ and μ) do not strongly depend on temperature but they seem to depend on the intrinsic properties of the amorphous phase. The background trap density is $\sim 10^{20}$ $\mathrm{at/cm^3}$ (see Table II), suggesting that these traps might be amorphous bulk defects, whose density in relaxed amorphous Si is known to be at most 1% at.[43] It is worth noting that the amorphous relaxation times (i.e., the time needed to defects to reach their equilibrium concentrations) extinguish in our samples well before than the a-c interfaces reach the F profiles at all the temperatures investigated.[44] The traps effective decay length at the a-c interface is ~ 150 nm, slightly increasing with the temperature. The equilibrium constant for trapping reaction (k) is $\sim 5 \times 10^{18}$ $\mathrm{at/cm^3}$ almost independent of temperature. The fact that the values found for the mobile F diffusivity D_{FI} coincides with the F diffusion coefficient measured by Nash *et al.* appears indeed quite surprising, as their diffusion coefficient represents the diffusion coefficient of the diffusive F, i.e., the D_{FD} in our model, that is different to the diffusion coefficient of the mobile F, D_{FI}, measured by us, that is the diffusivity of fraction of diffusive F not bonded to a trap. This is not an effect of different F concentrations, as they studied a similar F concentration regime than ours. The fact that the two different quantities coincide with each other can be understood within the framework of the present model by considering that the a-Si used in Ref. 18 has been produced by deposition, that is a considerably different method with respect to the one used for our samples. Their material might

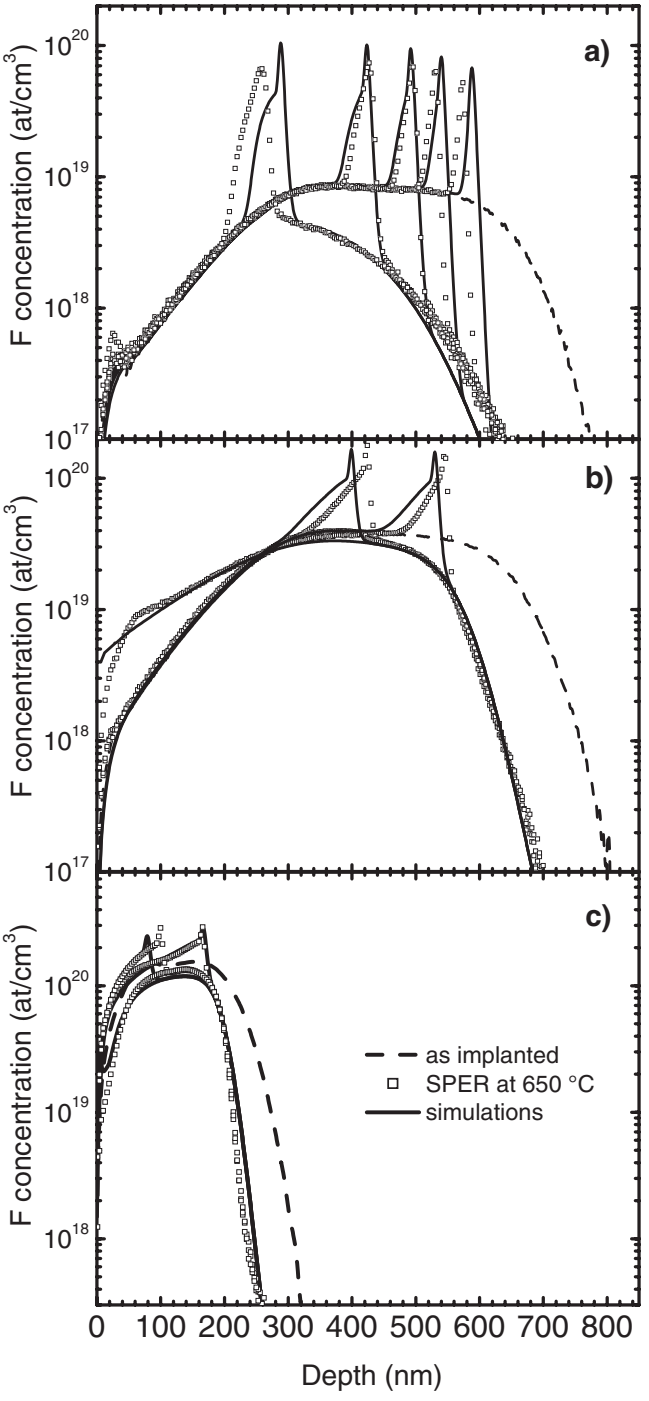

FIG. 9. F SIMS profiles just after implantation (dashed lines), during and after SPER at 650 °C (open squares) and best fit results (continuous lines) for: (a) LC samples (annealing times: 59, 89, 138, 252, and 583 s); (b) MC samples (annealing times: 290, 830, and 2930 s); (c) HCb samples (273, 826, and 1800 s).

therefore contain traps for mobile F at concentrations low enough for not having any significant influence on the F diffusion.

As outlined above, the F segregation at the interface region has a central role within the whole phenomenon. We found that by increasing the temperature the segregation factor α decreases while the releasing factor β increases by more than an order of magnitude. We estimated activation energies of α and β to be respectively (-0.8 ± 0.1) eV and (2.0 ± 1.1) eV [see Figs. 10(b) and 10(c)]. The negative value found for E_α indicates that the barrier of an F atom close to the a-c interface for "jumping" into the interface region is lower by (0.8 ± 0.1) eV than the barrier for diffusing back toward the amorphous phase. The positive value found for E_β indicates instead that there is a barrier of (2.0 ± 1.1) eV for the release of the F atoms from the interface region toward the amorphous phase, which is in agreement with the calculated binding energy of F to a dangling bond that is ~ 2 eV.[45,46] These values, together with the energy barrier discussed above for the F interstitial diffusivity, allow to draw the energy scheme reported in Fig. 11 describing the F diffusion in a-Si and its exchange between the amorphous phase and interface layer.

As shown previously, the above segregation mechanism governs also the retardation effect of F on the SPER rate, through the exponential law of Eq. (1) obtained directly from the experimental data. Consistently, the model allows to predict accurately the position of the a-c interface assuming the above exponential dependence, obtaining f_S^0 best fit parameters that are compatible within errors with the values obtained directly by the experimental data. The above exponential dependence is remarkable and allows the following interpretation.

There are experimental evidences reported in literature[26,47] that the SPER rate v has an exponential dependence on the stress state, σ_{ij}, through the relation

$$v = v_0 \exp\left(\frac{\Delta V_{ij}^* \sigma_{ij}}{kT}\right), \tag{24}$$

where v_0 is the stress-free velocity, kT has the usual meaning, i and j refer to axes in the coordinate frame of Ref. 47, and ΔV_{ij}^* represents the activation volume tensor. If we make the hypothesis that the segregated F produces a local stress (and consequently a strain) at the a-c interface, and that this stress is proportional to the amount of segregated F through the relation $\sigma_{ij}=p_{ij}f_S$, where p_{ij} is a tensor of forces, we obtain

$$v = v_0 \exp\left(\frac{\Delta V_{ij}^* p_{ij}}{kT} f_S\right). \tag{25}$$

The last equation is analytically identical to Eq. (1) allowing an interpretation of the exponential retardation of the SPER rate in terms of stress induced by the F in the interface layer. By comparing the Eq. (25) to Eq. (1) we get

$$\frac{f_S^0}{kT} = -\frac{1}{\Delta V_{ij}^* p_{ij}} \tag{26}$$

that indicates that the parameter f_S^0 divided by kT should be constant as a function of the temperature. This is what indeed happens as evidenced in Table II, supporting the validity of the above interpretation.

Further considerations can be made about the tensor p_{ij}. The epitaxial constraint imposes that the strain due to F builds up along the direction perpendicular to the a-c interface and the value of ΔV along this direction reported in

TABLE II. List of the optimized parameters at each annealing temperature.

	Model parameters		
	580 °C	650 °C	700 °C
D_{FI} (cm^2/s)	$(1.4 \pm 0.2) \times 10^{-14}$	$(1.2 \pm 0.2) \times 10^{-13}$	$(5.5 \pm 0.4) \times 10^{-13}$
k (at/cm^3)	$(7.3 \pm 0.5) \times 10^{18}$	$(3.1 \pm 0.5) \times 10^{18}$	$(4.2 \pm 1.6) \times 10^{18}$
T_{bulk} (at/cm^3)	$(6.7 \pm 0.1) \times 10^{19}$	$(8.7 \pm 2.0) \times 10^{19}$	$(1.4 \pm 0.3) \times 10^{20}$
μ (nm)	(84 ± 24)	(141 ± 30)	(169 ± 52)
α	$(1.3 \pm 0.2) \times 10^{-1}$	$(4.3 \pm 1.0) \times 10^{-2}$	$(3.1 \pm 0.4) \times 10^{-2}$
β (s^{-1})	$(3.6 \pm 0.5) \times 10^{-4}$	$(8.9 \pm 0.5) \times 10^{-4}$	$(9.5 \pm 0.9) \times 10^{-3}$
$\frac{f_S^0}{kT}$ (eV^{-1} cm^{-2})	$(4.1 \pm 0.1) \times 10^{14}$	$(2.7 \pm 0.1) \times 10^{14}$	$(3.0 \pm 0.1) \times 10^{14}$
N_0 (at/cm^3)	$(2.2 \pm 0.1) \times 10^{15}$	$(8.6 \pm 0.9) \times 10^{15}$	$(4.1 \pm 0.2) \times 10^{16}$
η (s^{-1})	$(2.5 \pm 1.8) \times 10^{-5}$	$(4.8 \pm 1.3) \times 10^{-3}$	$(8.4 \pm 0.8) \times 10^{-2}$

literature is negative.[27] Therefore, according to Eq. (26), the tensor p_{ij} along the same direction has to be positive, i.e., in order to explain the observed SPER rate reduction F should induce a dilatation of the crystal Si lattice in the direction perpendicular to the a-c interface. Strain depth profiles obtained by high resolution x-ray diffraction measurements (details on the measurement methodology can be found in Ref. 48) on selected samples have confirmed that in presence of F there is a dilatation of the lattice parameter close to the a-c interface along the direction perpendicular to it. As an example, in Fig. 12 the strain profiles of two samples are shown. The continuous line is related to a sample containing F and annealed at 650 °C for 273 s while the dashed line represents the strain profile of the same sample without F annealed at the same temperature for 42 s. As can be noted, two main features are visible in both strain profiles: the first one is the positive strain visible at the depth of ~550 nm that is a fingerprint of EOR defects[49] and it is nearly identical for both samples (the strain integral is the same within 3%); the second and more important feature is the positive strain located just beyond the a-c interface. It is clear that the strain increase is more pronounced when F is present in the sample (the ratio between the two maxima in the strain levels is about 5). This is a further confirmation of the above interpretation of a stress related SPER reduction induced by F.

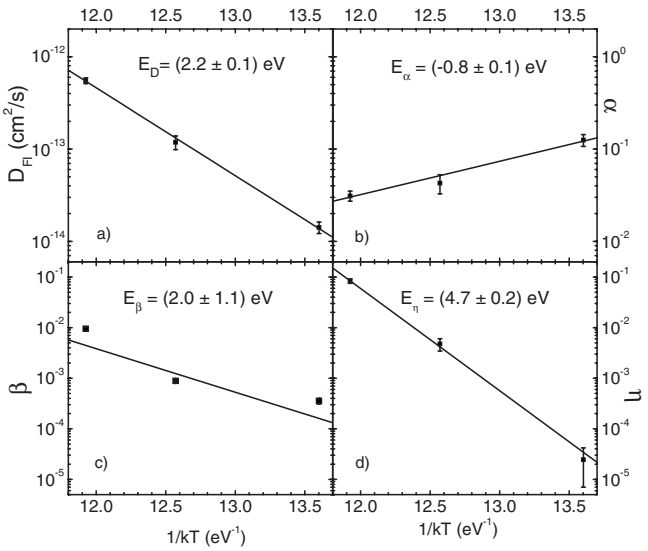

FIG. 10. Arrhenius plots for (a) the F the interstitial diffusivity D_{FI}, (b) the segregation factor α, (c) the releasing factor β, and (d) the cluster dissolution rate η.

The fact that our model simulates well the F incorporation tells that also the F clustering is modeled satisfactorily enough to account quantitatively for the F incorporation. However, a comparison with TEM measurement obtained in Ref. 34 in similar samples indicates that our model for clustering is indeed inaccurate in describing the details of the mechanisms involved nor in predicting the real cluster-size distributions and concentrations. In fact, contrary to what assumed in the model, the F clusters observed by TEM have not a unique radius but a considerably broad size distribution (from 0.5 to 4 nm). Moreover, as stated in Ref. 34, the F dose in the nanobubbles estimated by TEM represents a lower limit of the real value because nanobubbles with radius smaller than 0.5 nm fall below the TEM sensitivity, suggesting that the size distribution might be even broader than what indicated above. Presumably, various classes of clusters of different sizes and with a different content of F will exist simultaneously and their populations will vary with the temperature in a complex way. However, a more complex description of clustering than the one adopted, that considers a

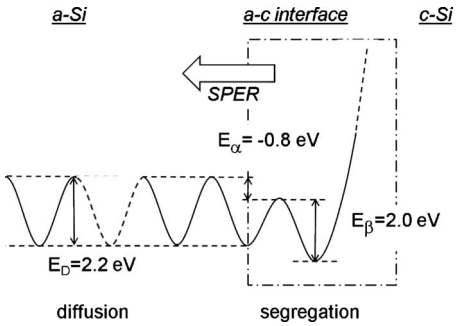

FIG. 11. Energy scheme for the F evolution in preamorphized Si during SPER close to the a-c interface. The involved mechanisms are represented by their energy barriers: E_D for the F diffusion in a-Si, E_α for the F segregation at the a-c interface region, and E_β for the release of F from the a-c interface region to bulk a-Si.

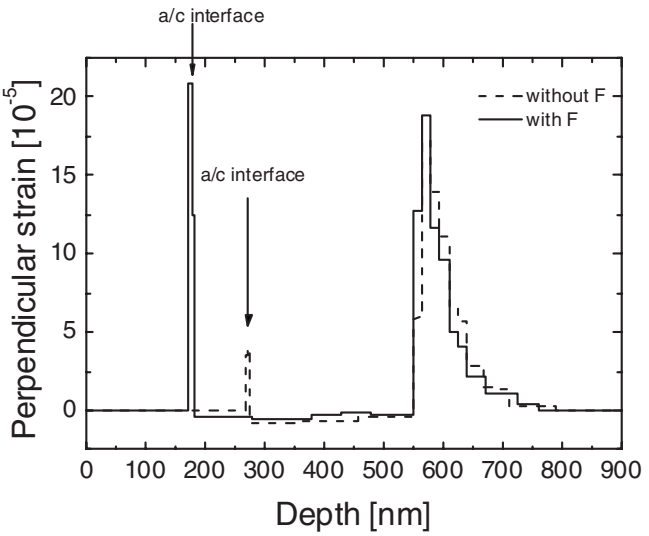

FIG. 12. Strain depth profile of sample HCb after annealing at 650 °C for 273 s obtained by high-resolution x-ray diffraction measurements (continuous line). The strain depth profile of the same sample without F and annealed at the same temperature for 42 s is shown for comparison (dotted line). The strain at the a-c interface is clearly much higher in the sample with F than in the sample without F. The strain due to the EOR defects is also visible at a depth of ~550 nm.

fixed concentration of clusters with a single value radius, would be beyond the sensitivity of the experimental procedure and beyond the scope of this work (the lack of sensitivity might be a consequence of the fact that in most of our samples the concentration of F in clusters is a small fraction of the total concentration F in a-Si). Due to the above considerations, we omit any detailed discussion on the values found for N_0. However, it is worth noting that the value of N_0 at 700 °C reported in Table II gives, through the Eq. (5), a maximum value for the radius of the clusters in sample HCa at 700 °C of 3.7 nm (the maximum value of the concentration of F in clusters $F_C^{max}=1.7\times10^{20}$ at/cm^3 extracted from the simulations was used for the calculation). This value falls within the range estimated by TEM analysis in Ref. 34 at the same temperature and in a sample similar to the ones considered in the above calculation.

Different considerations might hold concerning the cluster dissolution process. In fact, the cluster dissolution probability η changes with temperature with an activation energy of (4.7 ± 0.2) eV [see Fig. 10(d)]. This considerably high value is remarkable and is not too far from the Si-F bond energy of 5.73 eV.[50] This suggests that, even if the real cluster evolution is certainly much more complex than what considered by the present model, the dissolution process is governed by a single simple phenomenon, satisfactorily described by the model, that presumably is the destruction of the Si-F bond in the SiF_4 molecules.

VI. CONCLUSIONS

In conclusion, we have investigated and modeled the evolution and incorporation of F implanted in a-Si during SPER. The phenomenon is complex and involves at least four mechanisms relative to the F behavior mutually interacting, and all of them have been investigated and understood. We have demonstrated that the reduction in the SPER rate in the presence of F is governed only by the F areal density segregated at the a-c interface following a simple exponential decay. We have shown experimentally that F induces a positive strain perpendicular to the a-c interface and such strain accounts for the above SPER rate reduction by slowing the migration of the ledges responsible for the regrowth. The dynamics of the areal density of the F segregated at the a-c interface can be well described by a sticking-release model and the analysis of the related parameters allowed to fix the energy scheme of F close to the interface. This dynamics together with the exponential relation mentioned above allows to predict well the SPER velocity. Different models describing the F diffusion in the amorphous phase were tried, such as constant diffusion, concentration-dependent diffusion, etc. The most satisfactory and reasonable model assumes that F diffusion in a-Si is described by a trap-limited mechanism. We estimated that the diffusivity of mobile F in a-Si has an activation energy of (2.2 ± 0.1) eV, that is consistent with the value reported in literature,[18] and gave a microscopic interpretation of the F diffusion. We described the clustering of F in the amorphous phase by assuming a clustering rate proportional to the F concentration and the F diffusivity. Finally, a very good description of F incorporation in the crystalline phase can be reached by assuming that all the F precipitated in the amorphous phase is fully incorporated in c-Si after regrowth and that a negligible diffusion of F occurs in the crystal.

We described all these physical processes in a single overall model able to simulate the evolution of F chemical profiles in a wide range of concentrations and annealing temperatures. The above results give important insights on the microscopical mechanisms governing F redistribution and incorporation during SPER of preamorphized Si and also a powerful simulation tool for improving the fabrication of advanced USJs. Our modeling approach could be useful also in other similar systems in which redistribution of impurities during phase transition of the substrate occurs [e.g., H in Si (Ref. 51) or F in Ge during SPER].

ACKNOWLEDGMENTS

The authors wish to thank R. Storti (University of Padova), C. Percolla, and S. Tati (CNR-INFM MATIS, Catania) for their technical contributions. One of the authors (G.B.) wishes to thank CNISM for partial support.

*Corresponding author; napolitani@padova.infm.it
†Present address: IM2NP, case 142 Faculté Saint Jérôme 13397 Marseille, Cedex 20.

[1] The International Technology Roadmap for Semiconductors, 2007, www.itrs.net
[2] J. Y. Jin, J. Liu, U. Jeong, S. Metha, and K. Jones, J. Vac. Sci. Technol. B **20**, 422 (2002).
[3] B. J. Pawlak, R. Surdeanu, B. Colombeau, A. J. Smith, N. E. B. Cowern, R. Lindsay, W. Vandervost, B. Brijs, O. Richard, and F. Cristiano, Appl. Phys. Lett. **84**, 2055 (2004).
[4] L. Csepregi, J. W. Mayer, and T. W. Sigmon, Phys. Lett. A **54**, 157 (1975).
[5] S. Solmi, E. Landi, and F. Baruffaldi, J. Appl. Phys. **68**, 3250 (1990).
[6] C. Bonafos, D. Mathiot, and A. Claverie, J. Appl. Phys. **83**, 3008 (1998).
[7] F. Cristiano, N. Cherkashin, P. Calvo, Y. Lamrani, X. Hebras, A. Claverie, W. Lerch, and S. Paul, Mater. Sci. Eng., B **114-115**, 174 (2004).
[8] A. E. Michel, W. Rausch, P. A. Ronsheim, and R. H. Kastl, Appl. Phys. Lett. **50**, 416 (1987).
[9] K. S. Jones, L. H. Zhang, V. Krishnamoorthy, M. Law, D. S. Simmons, P. Chi, L. Rubin, and R. G. Elliman, Appl. Phys. Lett. **68**, 2672 (1996).
[10] E. Napolitani, A. Coati, D. De Salvador, A. Carnera, S. Mirabella, S. Scalese, and F. Priolo, Appl. Phys. Lett. **79**, 4145 (2001).
[11] S. Mirabella, A. Coati, D. De Salvador, E. Napolitani, A. Mattoni, G. Bisognin, M. Berti, A. Carnera, A. V. Drigo, S. Scalese, S. Pulvirenti, A. Terrasi, and F. Priolo, Phys. Rev. B **65**, 045209 (2002).
[12] M. Di Marino, E. Napolitani, M. Mastromatteo, G. Bisognin, D. De Salvador, A. Carnera, S. Mirabella, G. Impellizzeri, F. Priolo, H. Graoui, and M. A. Foad, Nucl. Instrum. Methods Phys. Res. B **253**, 46 (2006).
[13] D. F. Downey, J. W. Chow, E. Ishida, and K. S. Jones, Appl. Phys. Lett. **73**, 1263 (1998).
[14] H. A. W. El Mubarek, J. M. Bonar, G. D. Dilliway, P. Ashburn, M. Karunaratne, A. F. Willoughby, Y. Wang, P. L. F. Hemment, R. Price, J. Zhang, and P. Ward, J. Appl. Phys. **96**, 4114 (2004).
[15] G. Impellizzeri, J. H. R. dos Santos, S. Mirabella, F. Priolo, E. Napolitani, and A. Carnera, Appl. Phys. Lett. **84**, 1862 (2004).
[16] N. E. B. Cowern, B. Colombeau, J. Benson, A. J. Smith, W. Lerch, S. Paul, T. Graf, F. Cristiano, X. Hebras, and D. Bolze, Appl. Phys. Lett. **86**, 101905 (2005).
[17] G. Impellizzeri, S. Mirabella, F. Priolo, E. Napolitani, and A. Carnera, J. Appl. Phys. **99**, 103510 (2006).
[18] G. R. Nash, J. F. W. Schiz, C. D. Marsh, P. Ashburn, and G. R. Booker, Appl. Phys. Lett. **75**, 3671 (1999).
[19] S. Mirabella, G. Impellizzeri, E. Bruno, L. Romano, M. G. Grimaldi, F. Priolo, E. Napolitani, and A. Carnera, Appl. Phys. Lett. **86**, 121905 (2005).
[20] C. P. Ho, J. D. Plummer, S. E. Hansen, and R. W. Dutton, IEEE Trans. Electron Devices **28**, 1438 (1983).
[21] V. G. Smith, W. A. Tiller, and J. W. Rutter, Can. J. Phys. **33**, 723 (1955).
[22] J. Zhang, Y. Ashizawa, and H. Oka, Proc. IWJT. Tech. Dig., 2006, pp. 50–53.
[23] N. Zographos and I. Martin-Bragado, Mat. Res. Soc. Symp. Proc. **1070**, E03-01 (2008).
[24] G. L. Olson and J. A. Roth, Mater. Sci. Rep. **3**, 1 (1988).
[25] B. C. Johnson and J. C. McCallum, Phys. Rev. B **76**, 045216 (2007).
[26] N. G. Rudawski, K. S. Jones, and R. Gwilliam, Phys. Rev. Lett. **100**, 165501 (2008).
[27] N. G. Rudawski, K. S. Jones, and R. Gwilliam, Mater. Sci. Eng., R. **61**, 40 (2008).
[28] D. D'Angelo, L. Romano, I. Crupi, E. Carria, V. Privitera, and M. G. Grimaldi, Appl. Phys. Lett. **93**, 231901 (2008).
[29] J. A. Roth, G. L. Olson, D. C. Jacobson, and J. M. Poate, Appl. Phys. Lett. **57**, 1340 (1990).
[30] J. S. Williams and R. G. Elliman, Phys. Rev. Lett. **51**, 1069 (1983).
[31] B. Park, Jpn. J. Appl. Phys. **35**, L1611 (1996).
[32] N. G. Rudawski, K. S. Jones, S. Morarka, M. E. Law, and R. G. Elliman, J. Appl. Phys. **105**, 081101 (2009).
[33] G. Impellizzeri, S. Mirabella, A. M. Piro, M. G. Grimaldi, F. Priolo, F. Giannazzo, V. Raineri, E. Napolitani, and A. Carnera, Appl. Phys. Lett. **91**, 132101 (2007).
[34] S. Boninelli, G. Impellizzeri, S. Mirabella, F. Priolo, E. Napolitani, N. Cherkashin, and F. Cristiano, Appl. Phys. Lett. **93**, 061906 (2008).
[35] D. De Salvador, G. Bisognin, E. Napolitani, M. Mastromatteo, N. Baggio, A. Carnera, F. Boscherini, G. Impellizzeri, S. Mirabella, S. Boninelli, F. Priolo, and F. Cristiano, Appl. Phys. Lett. **95**, 101908 (2009).
[36] F. Lau, L. Mader, C. Mazure, Ch. Werner, and M. Orlowski, Appl. Phys. A: Mater. Sci. Process. **49**, 671 (1989).
[37] M. Orlowski, Appl. Phys. Lett. **55**, 1762 (1989).
[38] P. R. Bevington and D. K. Robinson, *Data Reduction and Error Analysis for the Physical Sciences*, XV ed. (McGraw-Hill, New York, 1969).
[39] S. T. Pantelides, Phys. Rev. Lett. **57**, 2979 (1986).
[40] G. N. van den Hoven, Z. N. Liang, L. Niesen, and J. S. Custer, Phys. Rev. Lett. **68**, 3714 (1992).
[41] X. Urli, C. L. Dias, L. J. Lewis, and S. Roorda, Phys. Rev. B **77**, 155204 (2008).
[42] S. Roorda, W. C. Sinke, J. M. Poate, D. C. Jacobson, S. Dierker, B. S. Dennis, D. J. Eaglesham, F. Spaepen, and P. Fuoss, Phys. Rev. B **44**, 3702 (1991).
[43] S. Coffa, F. Priolo, and A. Battaglia, Phys. Rev. Lett. **70**, 3756 (1993).
[44] P. A. Stolk, F. W. Saris, A. J. M. Berntsen, W. F. van der Weg, L. T. Sealy, R. C. Barklie, G. Krötz, and G. Müller, J. Appl. Phys. **75**, 7266 (1994).
[45] V. Fiorentini and G. M. Lopez, Phys. Rev. Lett. **96**, 039601 (2006).
[46] M. Diebel and S. T. Dunham, Phys. Rev. Lett. **96**, 039602 (2006).
[47] M. J. Aziz, P. C. Sabin, and G.-Q. Lu, Phys. Rev. B **44**, 9812 (1991).
[48] G. Bisognin, D. De Salvador, E. Napolitani, A. Carnera, E. Bruno, S. Mirabella, F. Priolo, and A. Mattoni, Semicond. Sci. Technol. **21**, L41 (2006).
[49] G. Bisognin, S. Vangelista, and E. Bruno, Mater. Sci. Eng., B **154-155**, 64 (2008).
[50] *Handbook of Chemistry and Physics*, 71st ed., edited by D. R. Lide (CRC Press, Boston, 1990), pp. 9-86–9-89.
[51] J. A. Roth, G. L. Olson, D. C. Jacobson, J. M. Poate, and C. Kirschbaum, Mat. Res. Soc. Symp. Proc. **205**, 45 (1992).